Research article JHEP|Reports

Single-cell landscape of immune cells in human livers affected by HBV-related cirrhosis

Authors

Qingquan Bai, Xiaoting Hong, Han Lin, Xiao He, Runyang Li, Mohsin Hassan, Hilmar Berger, Frank Tacke, Cornelius Engelmann, Tianhui Hu

Correspondence

frank.tacke@charite.de (F. Tacke), cornelius.engelmann@charite.de (C. Engelmann), thu@xmu.edu.cn (T. Hu).

Graphical abstract

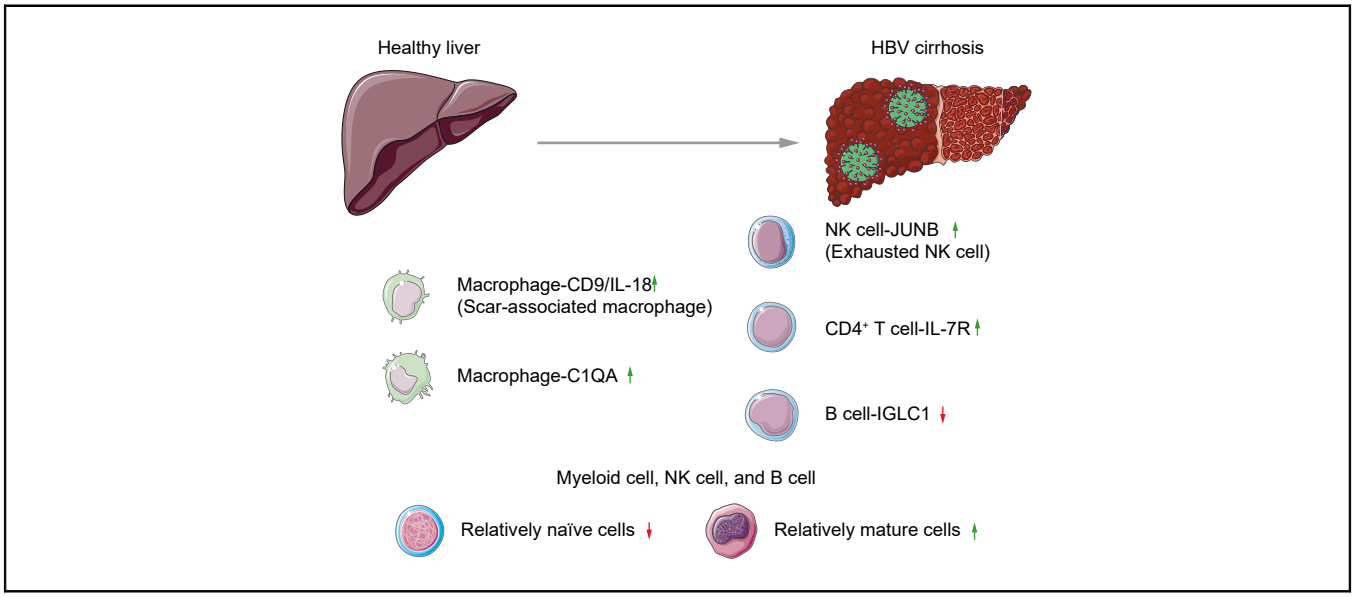

Highlights

- Scar-associated macrophage populations with distinct marker genes were expanded in HBV cirrhosis.
- Exhausted NK cells (NK cell-JUNB) are notably increased in HBV cirrhosis.
- Accumulation of relatively mature cells and loss of relatively naive cells was observed in myeloid, NK, and B cell subsets in HBV cirrhosis.
- Induction of antigen processing and presentation capacities was observed in myeloid cells in HBV cirrhosis.
- NK cell-mediated cytotoxicity is substantially diminished in HBV cirrhosis.

Impact and implications

The absence of single-cell transcriptome profiling of immune cells in HBV cirrhosis hinders our understanding of the underlying mechanisms driving disease progression. To address this knowledge gap, our study unveils a distinctive immune ecosystem in HBV cirrhosis and represents a crucial advancement in elucidating the impact of the immune milieu on the development of this condition. These findings constitute significant strides towards the identification of more effective therapeutic approaches for HBV cirrhosis and are relevant for healthcare professionals, researchers, and pharmaceutical developers dedicated to combating this disease.

https://doi.org/10.1016/j.jhepr.2023.100883

Research article

JHEP|Reports

Single-cell landscape of immune cells in human livers affected by HBV-related cirrhosis

Qingquan Bai,[1,2,3,†] **Xiaoting Hong**,[1,†] **Han Lin**,[4,†] Xiao He,[5] Runyang Li,[1,2] Mohsin Hassan,[3] Hilmar Berger,[3] Frank Tacke,[3,*] Cornelius Engelmann,[3,6,7,*] Tianhui Hu[1,2,8,*]

[1]*Cancer Research Center, School of Medicine, Xiamen University, Xiamen, China;* [2]*National Institute for Data Science in Health and Medicine, Xiamen University, Xiamen, China;* [3]*Department of Hepatology & Gastroenterology, Charité Universitätsmedizin Berlin, Campus Virchow-Klinikum and Campus Charité Mitte, Berlin, Germany;* [4]*Department of Hepatic Surgery, The First Affiliated Hospital of Harbin Medical University, Harbin, China;* [5]*Department of Neurology, The First Affiliated Hospital of Shandong First Medical University, Jinan, China;* [6]*Berlin Institute of Health, Charité-Universitätsmedizin Berlin, Berlin, Germany;* [7]*Institute for Liver and Digestive Health, University College London, Royal Free Campus, London, UK;* [8]*Shenzhen Research Institute, Xiamen University, Shenzhen, China*

JHEP Reports **2023.** https://doi.org/10.1016/j.jhepr.2023.100883

Background & Aims: HBV infection is one of the leading causes of liver cirrhosis. However, the immune microenvironment in patients with HBV cirrhosis remains elusive.
Methods: Single-cell RNA sequencing was used to analyse the transcriptomes of 76,210 immune cells in the livers of six healthy individuals and in five patients with HBV cirrhosis.
Results: Patients with HBV cirrhosis have a unique immune ecosystem characterised by an accumulation of macrophage-CD9/IL18, macrophage-C1QA, NK Cell-JUNB, CD4$^+$ T cell-IL7R, and a loss of B cell-IGLC1 clusters. Furthermore, our analysis predicted enhanced cell communication between myeloid cells and all immune cells in patients with HBV-related cirrhosis. Pseudo-time analysis of myeloid cells, natural killer (NK) cells, and B cells demonstrated a significant accumulation of mature cells and a depletion of naive cells in HBV cirrhosis. In addition, we observed an increase in antigen processing and presentation capacities in myeloid cells in patients with HBV cirrhosis, whereas NK cell-mediated cytotoxicity was substantially reduced.
Conclusions: Our results provide valuable insight into the immune landscape of HBV cirrhosis, suggesting that HBV cirrhosis is associated with the accumulation of activated myeloid cells and impaired cytotoxicity in NK cells.
Impact and implications: The absence of single-cell transcriptome profiling of immune cells in HBV cirrhosis hinders our understanding of the underlying mechanisms driving disease progression. To address this knowledge gap, our study unveils a distinctive immune ecosystem in HBV cirrhosis and represents a crucial advancement in elucidating the impact of the immune milieu on the development of this condition. These findings constitute significant strides towards the identification of more effective therapeutic approaches for HBV cirrhosis and are relevant for healthcare professionals, researchers, and pharmaceutical developers dedicated to combating this disease.

Introduction

Liver cirrhosis is one of the most relevant chronic diseases endangering public health. Globally, more than one million individuals died of liver cirrhosis in 2017,[1] and chronic HBV infection is one of the leading causes of cirrhosis, especially in Asia.[2]

The liver functions as an important constituent of the immune system. Complex interactions between immune cells contribute to the progression of liver cirrhosis. Different immune cell subsets, including lymphocytes and myeloid cells, cause inflammation and tissue injury, which are critical events during the development of liver cirrhosis.[3] Although immunological insights into the pathogenesis of liver cirrhosis arising from non-alcoholic fatty liver disease, alcoholic injury, and primary biliary cholangitis have been made,[4] our understanding of HBV-associated cirrhosis remains limited. Existing reports have predominantly focused on characterising the immune microenvironment in HBV infection and HBV-associated hepatocellular carcinoma.[5,6]

The development of high-throughput RNA sequencing at the single-cell level has revolutionised transcriptome analysis. Single-cell RNA sequencing (scRNA-seq) offers novel approaches for resolving the complexity and heterogeneity of immune cells, enabling the identification of novel cell subsets and the

Keywords: Cirrhosis; Hepatitis B; Immune cell; Liver; Single-cell RNAseq.
Received 30 December 2022; received in revised form 15 July 2023; accepted 22 July 2023; available online 18 August 2023
† These authors contributed equally to this work.
* Corresponding authors. Addresses: Department of Hepatology & Gastroenterology, Charité Universitätsmedizin Berlin, Campus Virchow-Klinikum and Campus Charité Mitte, 13353 Berlin, Germany (F. Tacke); Department of Hepatology & Gastroenterology, Charité Universitätsmedizin Berlin, Campus Virchow-Klinikum and Campus Charité Mitte, 13353 Berlin, Germany (C. Engelmann); Cancer Research Center, School of Medicine, Xiamen University, Xiamen, 361102 Fujian, China (T. Hu). Charite: Tel. +49 30 450 553022; Fax +49 30 450 553902.
E-mail addresses: frank.tacke@charite.de (F. Tacke), cornelius.engelmann@charite.de (C. Engelmann), thu@xmu.edu.cn (T. Hu).

exploration of underlying cell lineage relationships.[7] In this study, we used scRNA-seq to construct an unbiased and comprehensive atlas of intrahepatic immune cells and compared the changes in immune cells in the livers of healthy individuals and patients with HBV cirrhosis. The exact dissection of the contribution of immune cells to liver cirrhosis could provide new clues to develop novel therapeutic targets for HBV-associated liver cirrhosis.

Patients and methods

Study participants

The study was approved by the Ethics Review Center of the First Affiliated Hospital of Harbin Medical University (No. 2021179). Liver tissue was collected from orthotopic liver transplantations conducted at the Department of Liver Surgery of the First Affiliated Hospital of Harbin Medical University between 1 March 2021 and 30 September 2021. The sample cohort consisted of two healthy donors and two patients diagnosed with HBV cirrhosis. Healthy samples consisted of small specimens used for assessing organ quality before liver transplantation. Informed consent was obtained from all the patients and donors involved in the study. Single-cell transcriptome data from a total of 45,993 immune cells were acquired from these samples. Additionally, we acquired single-cell transcript transcriptome data from four healthy livers (19,389 cells) sourced from HRA001730 (a study on HBV infection)[6] and three HBV cirrhotic livers (10,828 cells) sourced from HRA000069 (a study on HBV related cancer development),[8] with the permission from China National Center for Bioinformation (CNCB). The clinical characteristics of these patients are summarised in Table S1. Overall, a total of 76,210 immune cells from healthy livers (n = 6) and HBV cirrhotic livers (n = 5) were analysed.

Human tissue processing

During the surgical procedure, wedge biopsies of non-ischemic fresh liver tissue (~2–3 g per liver) were collected before interrupting hepatic vascular inflow. The collected liver tissue was immediately immersed in a pre-cooled DMEM medium (Gibco, 11965092, New York, USA) at 4 °C and transported to a sterile laboratory bench within 5 min for further processing. The tissue was washed with phosphate-buffered saline (PBS, Gibco, 14190094, New York, USA) three times and cut into small pieces of approximately ~1–3 mm^3 size. The samples were suspended in a cryopreservation solution (10% dimethylsulfoxide, Sigma, D8418, Shanghai, China) in 90% foetal bovine serum (Gibco, 10100147, New South Wales, Australia), and stored at -80 °C until thawed and utilised for single-cell sequencing analysis within 5 days.

Tissue dissociation and cell sorting

Single-cell suspensions from tissues were prepared using a multi-tissue dissociation kit (MACS, 130110201, Bergisch Gladbach, Germany) according to the manufacturer's instructions. Briefly, the tissue samples were thawed at 37 °C and washed twice with DMEM before being minced and digested in a gentleMACS™ C tube (MACS, Bergisch Gladbach, Germany) containing digestion solution (4.7 ml of DMEM, 200 μl Enzyme D, 25 μl Enzyme A, and 100 μl Enzyme R [MACS, Bergisch Gladbach, Germany]) for 30 min at 37 °C. The cell suspension was passed through a 40 μm cell strainer (Corning, 431750, New York, USA) and centrifuged at 500 × *g* for 5 min. The cell pellet was resuspended in red blood cell lysis buffer (QIAGEN, 8570396, California, USA) and incubated on ice for 3 min. The suspension was centrifuged at 500 × *g* for 5 min at 4 °C, resuspended in PBS, and further processed for cell sorting.

To obtain haematopoietic cells, the suspension was stained with PerCP-Cyanine5.5 conjugated CD45 monoclonal antibody (Invitrogen, 45045941, New York, USA), and propidium iodide (PI) (Invitrogen, BMS500PI, New York, USA) dye. The stained cells were washed twice with DMEM medium containing 10% serum and sorted by fluorescence-activated cell sorting (FACS) (Sony, SH800S, Tokyo, Japan).

ScRNA-seq based on droplet generation

For scRNA-seq, cells were processed through the 10X Genomics single cell platform using the Next GEM Single cell v3.1 library kit (10X Genomics, PN-1000157, California, USA), Next GEM Gel Beads v3.1 (10X Genomics, PN-2000164, California, USA), and Next GEM chip G (10X Genomics, PN-2000177, California, USA). Approximately 16,000 cells for each sample were loaded onto 10X Chromium chips, and around 8,000–10,000 cells were captured. Gel beads with barcodes, single cells, and primers were wrapped in oil droplets to form the gel beads in emulsion emulsions. cDNA libraries with barcode and unique multiplex index (UMI) information for sequencing was generated by reverse transcription of the mRNA. The cDNA libraries were subjected to sequencing using the MGISEQ-2000 sequencing platform.

Dataset integration and batch effect removal

We integrated our scRNA-Seq dataset with datasets from two previous studies[6,8] and removed batch effect using integration anchors as implemented in Seurat.[9] Dataset integration, batch effect removal, and subsequent downstream analysis followed the standard Seurat workflow.

Analysis software

The following software was used for analysis: Cell Ranger 4.0, for data comparison, cell identification, and gene quantification; Seurat 3.2,[9] for cell clustering and marker gene identification: Doubletfinder 2.0.3,[10] for double cell removal; Velocyto 0.17.17,[11] for RNA rate change analysis; Reactome 1.26.0,[12] for gene enrichment analysis; Gsva 1.37.5,[13] gene variation analysis; GSEA 4.1.0,[14,15] for gene enrichment analysis; CellChat 1.6.1,[16] for cell–cell communication analysis; monocle 2.22.0,[17,18] for pseudotime analysis.

Immunofluorescence

The slides with liver sections were placed in an oven (Haiyiheng Scientific Instruments, PH-070A, Shanghai, China) and baked at a constant temperature of 63 °C for 2 h. Deparaffinisation was then performed using xylene, followed by gradual rehydration with a series of ethanol solutions. Antigen retrieval was performed by microwave heating in antigen retrieval solution (DAKO, Cambridgeshire, UK). Subsequently, sections were blocked with 10% goat serum in PBS for 10 min. After washing with PBS, the sections were incubated with primary antibodies (Table S2) at 4 °C overnight, followed by incubation with Cy3 or FITC conjugated secondary antibodies for 20 min at room temperature. The sections were counterstained with DAPI (Thermo Scientific, 62248, New York, USA) for 10 min at room temperature and mounted with the VECTASHIELD hardest antifade mounting medium (Vector Labs, H-1400, California, USA). Full scans were visualised

with a Tissue FAXS viewer (Tissue Gnostics, Vienna, Austria), and five different images were randomly selected from each sample. The number of positive cells in each image was counted and averaged for statistical analysis.

Results

Single-cell atlas of immune cells in healthy and HBV cirrhotic human livers

We isolated CD45$^+$ leucocytes by FACS and obtained single-cell transcriptome data from 45,993 immune cells. By integrating these datasets with those from two previous studies[6,8] using Seurat software, we analysed a total of 76,210 immune cells derived from healthy livers (n = 6) and livers with HBV cirrhosis (n = 5).

Principal component analysis (PCA), followed by dimensionality reduction using the Uniform Manifold Approximation and Projection (UMAP) algorithm with 15 principal components was performed. Twenty-three cell clusters were identified based on the most significant marker genes (Fig. 1A and Fig. S1A) and classified into four major cell subtypes: T cells (CD4+/CD8A+/CD8B+), myeloid cells (CD14+/FCGR3A+), NK cells (KLRF1+), and B cells (CD19+) (Fig. 1B). To assess potential differences between healthy and HBV-cirrhotic liver tissues, a comparative analysis was conducted, as illustrated in Fig. 1C. No significant variations were observed in the proportions of the four major cell subtypes between the two groups. Furthermore, Fig. 1D displays the most significant marker genes associated with each subcluster, providing valuable insights into their distinct molecular signatures. The contamination rate of non-haematopoietic cells, encompassing cycling cells, mesenchymal cells, and hepatocytes, was determined to be low, representing a mere 2.8% of the total cell count.

Enhanced antigen processing and presentation in myeloid cells during HBV cirrhosis

Myeloid cells are involved in the progression and sustenance of hepatic disorders across multiple stages.[19] We performed differential expression analysis of myeloid cells comparing healthy and HBV cirrhotic liver samples. A total of 489 genes were upregulated and 718 genes were downregulated in myeloid cells from HBV cirrhotic livers (Table S3 and Fig. S1B). GSEA analysis of myeloid cells with annotation pathway from Gene Ontology (GO) database showed that chromatin and cellular response to reactive oxygen species was inhibited, whereas antigen binding, positive regulation of T cell mediated immunity, and antigen processing and presentation of peptide or polysaccharide antigen via MHC class II were promoted in HBV cirrhosis (Fig. S1C). Similarly, utilising annotation pathway from Kyoto Encyclopaedia of Genes and

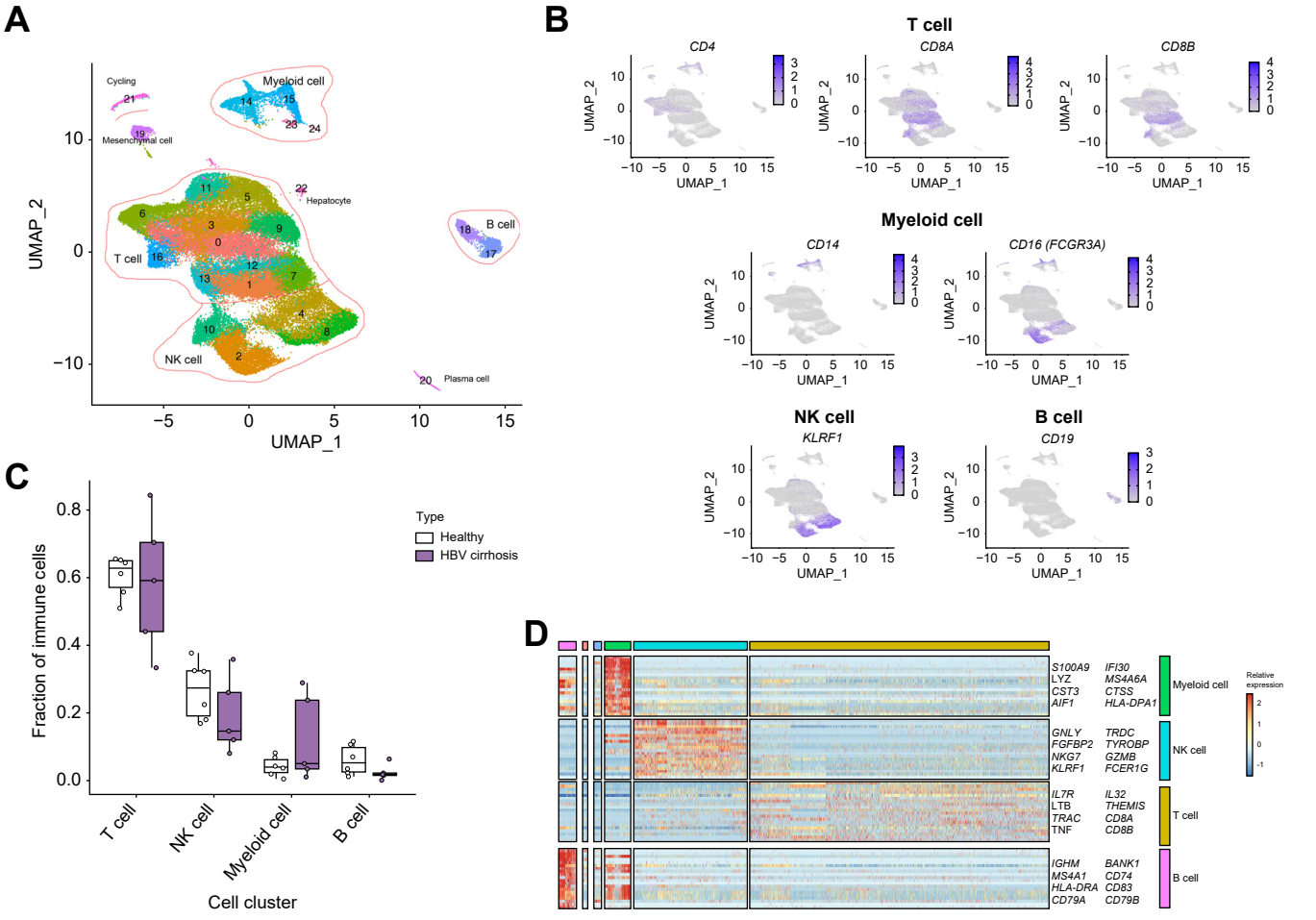

Fig. 1. Single-cell atlas of HBV cirrhotic and healthy livers. (A) Clustering analysis of all CD45$^+$ leucocytes. (B) UMAP plot showing the expression of *CD4, CD8A, CD8B, CD14, CD19, FCGR3A(CD16),* and *KLRF1.* (C) The proportion of T cells, NK cells, myeloid cells, and B cells in healthy liver and HBV cirrhotic liver samples. (D) Gene expression heatmap in each cell cluster. NK, natural killer; UMAP, Uniform Manifold Approximation and Projection.

Genomes (KEGG) database, GSEA analysis demonstrated that antigen processing and presentation were induced, and the MAPK signalling pathway was inhibited in HBV cirrhosis myeloid cells (Fig. S1C).

Macrophage-C1QA and macrophage-CD9/IL18 expanded in HBV cirrhosis

We conducted an in-depth analysis of myeloid subsets. A total of 13 subclusters were identified, including macrophages, monocytes, and dendritic cells (Fig. 2C), and the proportion of each myeloid cell subcluster was compared between healthy liver and HBV cirrhosis specimens (Fig. 2D and E, Fig. S1D).

Three monocyte subclusters were identified according to their crucial marker genes: Monocyte-S100A9, Monocyte-S100A6, and Monocyte-FCGR3A (Fig. 2A and B). Monocyte-S100A9 and Monocyte-S100A6 were considered as CD14+ classical monocyte, enriched in the expression of *S100A4, S100A6, S100A9*, and *S100A11* (Fig. 2C). Classical monocytes are known for their phagocytic activity.[20] Monocyte-FCGR3A, characterised by high *FCGR3A* (CD16) expression, was classified as non-classical CD16+ monocyte (Fig. 2C).

Macrophages were further clustered into seven subpopulations according to characteristic marker gene expression, and defined as Macrophage-CD9/IL18, Macrophage-CD9/IFI6,

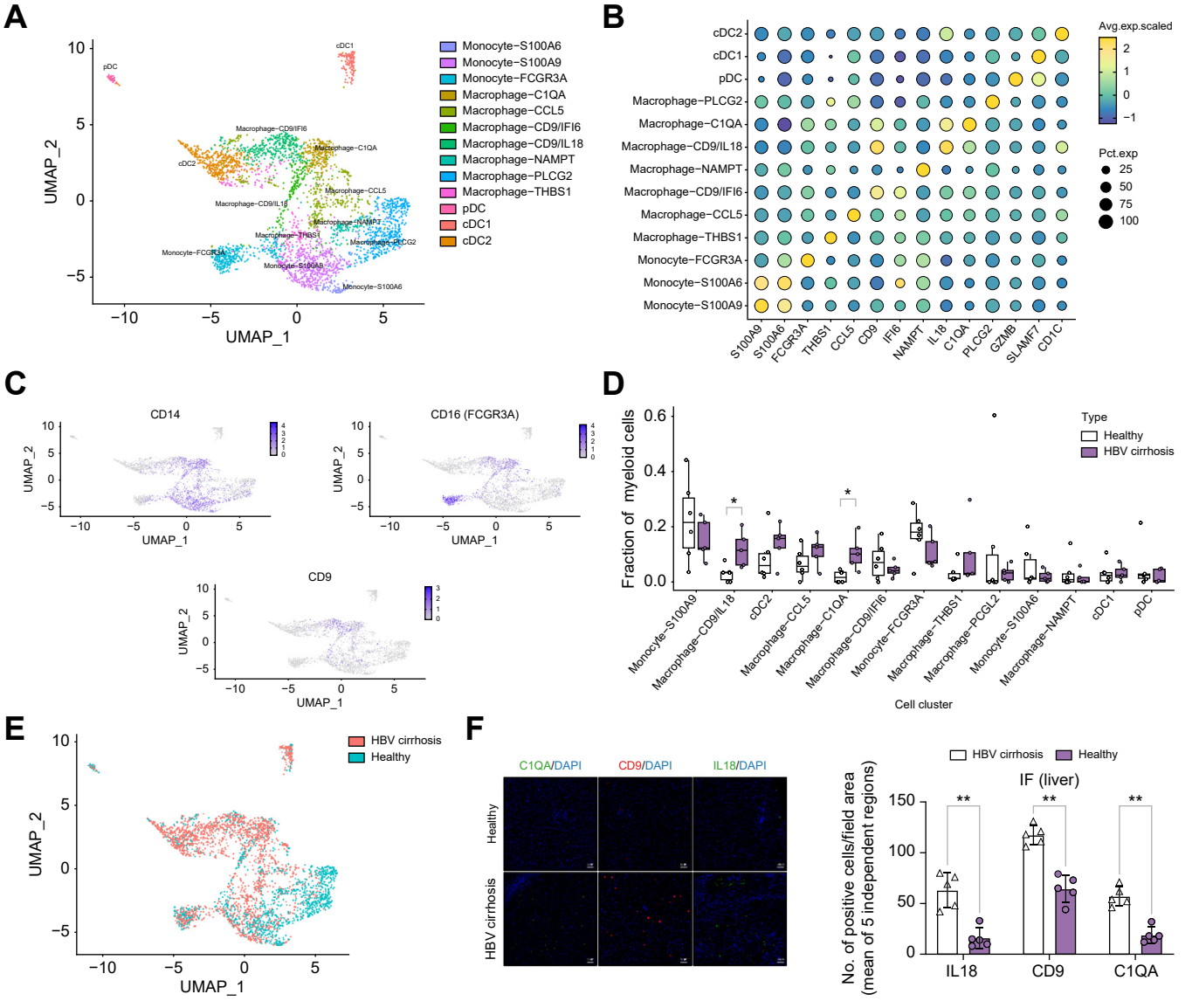

Fig. 2. The subtypes of myeloid cells in healthy and HBV cirrhotic livers. (A) Clustering analysis of all myeloid cells. (B) Dot plot illustrating the expression of marker genes in each cluster. (C) The expression of *CD14, FCGR3A(CD16),* and *CD9* in the UMAP plot. (D) The proportion of different clusters in myeloid cells in healthy and HBV cirrhotic livers. **p* <0.05 (Mann–Whitney *U* test). (E) UMAP plots of the distribution of major cell clusters in healthy and HBV cirrhotic liver samples. (F) Immunofluorescence images showing *C1QA, CD9*, and *IL18* expression in healthy and HBV cirrhotic livers samples (left panel). Quantification of positive cells from immunofluorescent images, ***p* <0.01 (right panel). (G) GO and KEGG enrichment analysis of Monocyte-C1QA and Macrophage-CD9/IL18 marker genes. (H) Differential expression of pro-inflammatory and anti-inflammatory genes between healthy and HBV cirrhosis in clusters of macrophages and monocytes. **p* <0.05, ***p* <0.01, ***p <0.001 (Mann-Whitney *U* test). GO, Gene Ontology; KEGG, Kyoto Encyclopaedia of Genes and Genomes; NK, natural killer; UMAP, Uniform Manifold Approximation and Projection.

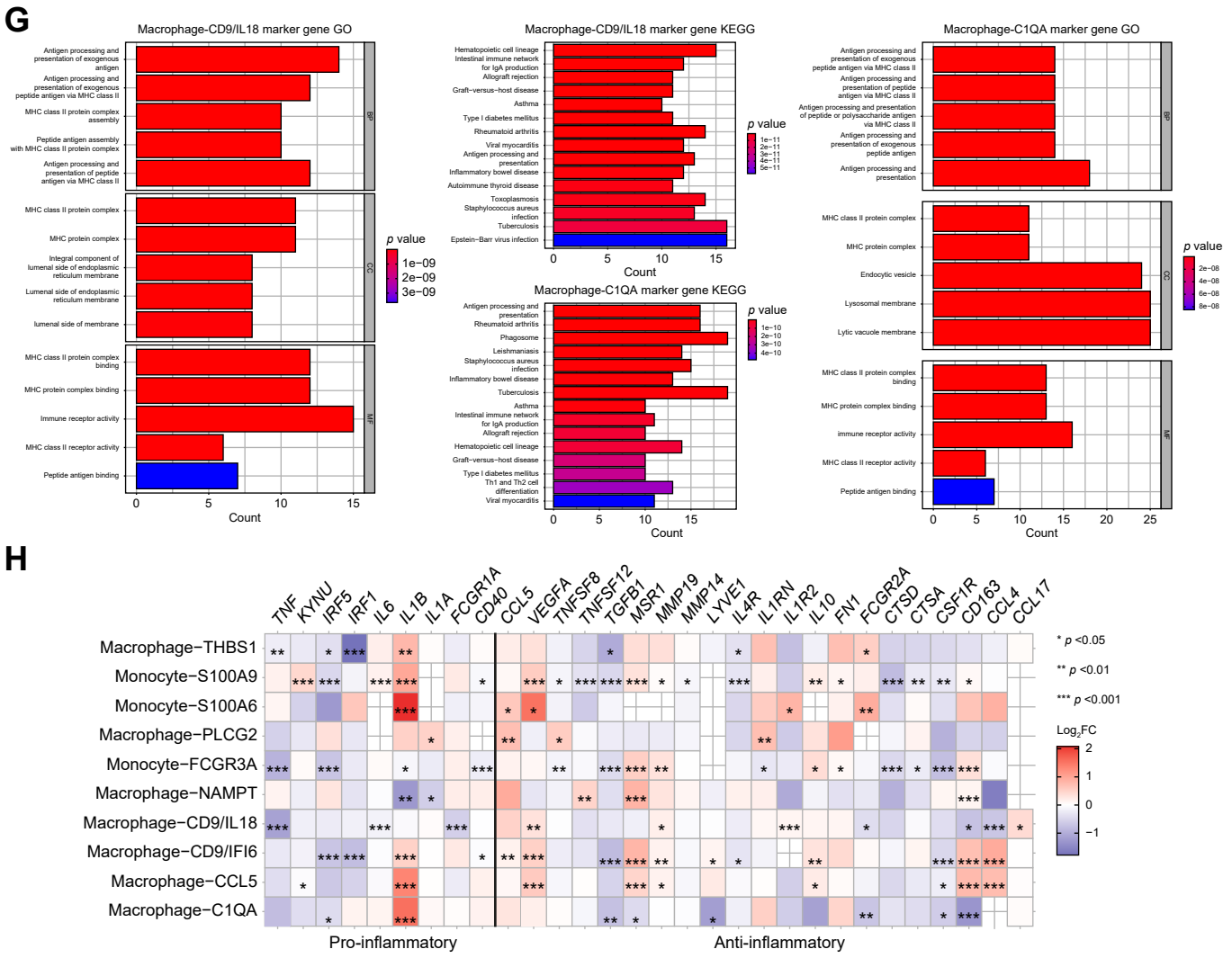

Fig. 2 (*continued*).

Macrophage-NAMPT, Macrophage-CCL5, Macrophage-PLCG2, Macrophage-THBS1, and Macrophage-C1QA (Fig. 2A and B). Macrophage-CD9/IL18 and Macrophage-CD9/IFI6 shared the same marker gene *CD9*. Previous studies have identified a CD9-enriched macrophage subcluster termed as scar-associated macrophages, which expands and resides in the fibrotic niche in liver cirrhosis unrelated to viral hepatitis.[4] Consistent with this, we found that Macrophage-CD9/IL18 increased in HBV cirrhosis samples (p <0.05) (Fig. 2D and E). C1QA encodes the A-chain polypeptide of serum complement subcomponent C1q.[21] The proportion of Macrophage-C1QA was increased in HBV cirrhosis samples (p <0.05) (Fig. 2D and E). Immunofluorescence staining validated the expansion of C1QA, CD9, and IL18 positive cells in HBV cirrhosis (Fig. 2F). To elucidate the functional characteristics of these two upregulated macrophage subclusters in HBV cirrhosis, Macrophage-CD9/IL18, and Macrophage-C1QA, we performed KEGG and GO pathway enrichment analysis on their marker genes. The results revealed that the phenotype of Macrophage-CD9/IL18 and Macrophage-C1QA was characterised by MHC class II, immune receptor activity, as well as antigen processing and presentation, suggesting the critical anti-viral immunity roles of these two elevated macrophage subclusters (Fig. 2G, Tables S4 and S5).

To define the inflammatory state of the myeloid subclusters, we examined the differential expression of ten pro-inflammatory genes and 20 anti-inflammatory genes. The fold change (log2) in gene expression levels in HBV cirrhotic livers compared to healthy livers was visualised using a heatmap (Fig. 2H). In the non-classical monocyte subcluster, Monocyte-FCGR3A, we observed downregulation of four pro-inflammatory genes and no upregulation, indicating that the pro-inflammatory effect of non-classical monocytes declined in HBV cirrhosis. In contrast, the anti-inflammatory effect of Macrophage-CD9/IL18 and Macrophage-C1QA were attenuated.

Enhanced CD74/CXCR4 signalling pathway on myeloid cells in HBV cirrhosis

To investigate the potential intercellular crosstalk among immune cells in HBV cirrhosis, cellular communication was predicted by using Cellchat. Notably, an increase in myeloid cell communication with all immune cells was predicted in HBV cirrhosis (Fig. 3A). The communication of different myeloid

subsets was then examined, and the results revealed that increased interactions with other immune cells was largely evident in Macrophage-C1QA and Macrophage-CCL5 subsets (Fig. 3B). Communication with other immune cells was largely reduced in plasmacytoid dendritic cells (pDCs) and slightly decreased in NK cells (Fig. 3B), which was in accordance with earlier findings that chronic HBV infection causes functional defects in pDCs and NK cells.[22,23] We also found that CD74/CXCR4 receptors in myeloid cells were activated by macrophage migration inhibitory factor (MIF) in HBV cirrhosis (p <0.05) (Fig. 3C). MIF binds to the CD74/CXCR4 complex, activating the ERK1/2 and AKT pathways via G-protein and promoting chemotaxis.[24,25]

Myeloid cells differentiated towards activated cell subsets in HBV cirrhosis

To explore the ontogeny and potential route of differentiation of myeloid cells in HBV cirrhosis, we performed pseudo-time and RNA velocity analyses (Fig. 4A and B). The results demonstrated that Monocyte-S100A6, Monocyte-S100A8, and Monocyte-

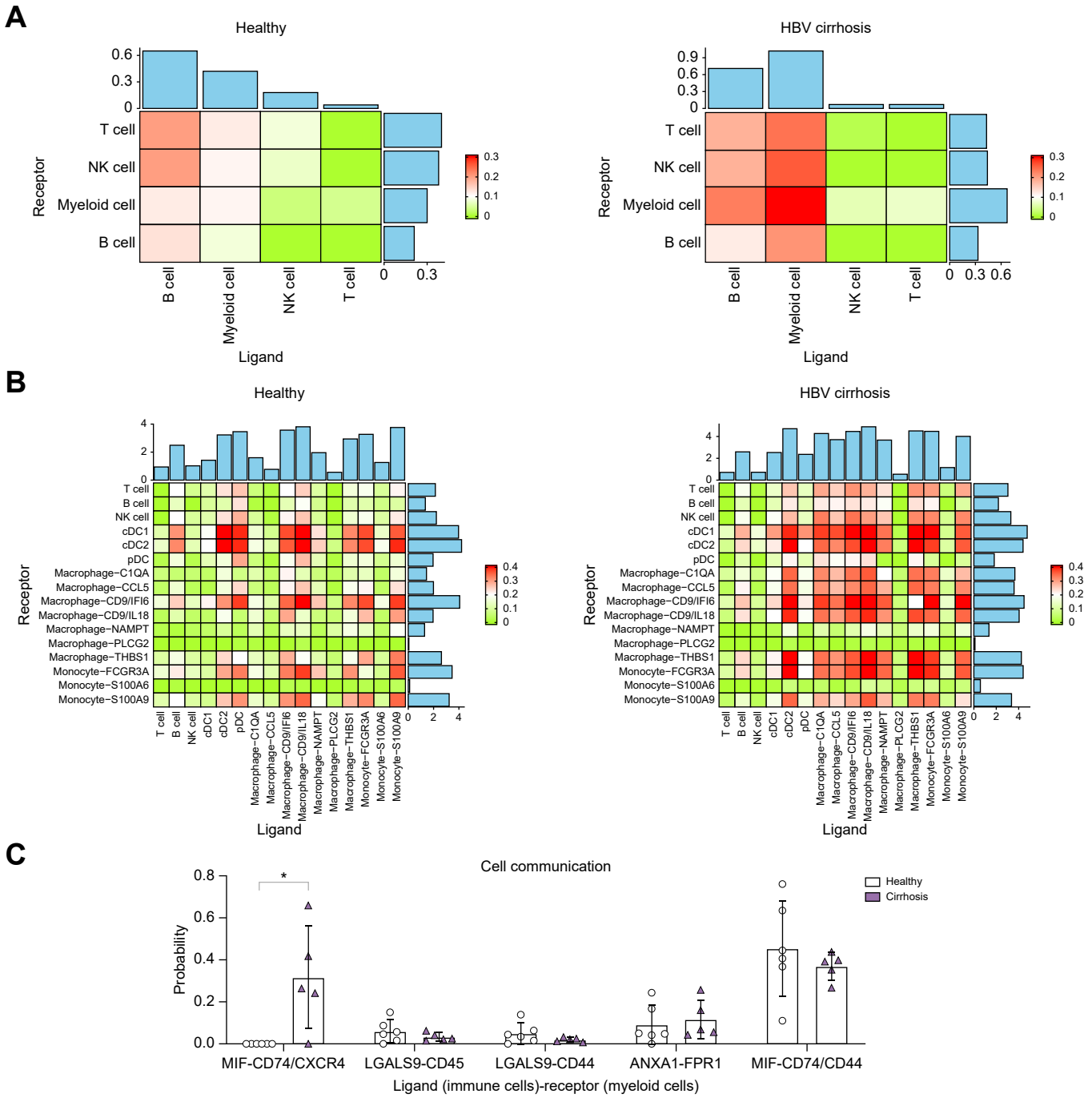

Fig. 3. Cell communication analysis of myeloid cells. (A) The strength of cell communication of immune cells in the healthy liver and HBV cirrhosis. (B) The strength of cell communication of myeloid cell subclusters in the healthy liver and HBV cirrhosis. (C) Cell communication of myeloid cell receptors and immune cell ligands $^{*}p$ <0.05, $^{**}p$ <0.01, $^{***}p$ <0.001 (Wilcoxon test).

FCGR3A exhibited a relatively immature phenotype, whereas Macrophages, pDC, cDC1, and cDC2 were classified as mature subsets (Fig. 4C and D). Among the various subsets of macrophages, Macrophage-PLCG2 and Macrophage-NAMPT represent the final differentiation of myeloid cells. Pseudo-time and RNA velocity analyses revealed a shift from immature (Monocyte-S100A6, Monocyte-S100A8, and Monocyte-FCGR3A) to mature (macrophage and dendritic cell subsets) in HBV cirrhosis (Fig. 4E and Fig. S1E), suggesting that myeloid cells differentiated into mature subgroups as HBV cirrhosis progressed.

We identified four distinct gene sets associated with myeloid cells differentiation as HBV cirrhosis progressed (Fig. 4F). Set 1 consists of markers for complement activation (*C1QA, C1QB, C1QC*) and antigen presentation (*HLA-DQB1*), which are macrophage and DC cell markers. Set 2 contained ribosomal protein (*RPS10, RPS11, RPL31*) and eukaryotic translation elongation factor (*EEF1B2*, *EEF1A1*), which are involved in cellular function like mRNA transcription and translation. The marker gene for final differentiations of myeloid cells, *PLCG2*, was also included in Set 3. Set 4 included myeloid cell precursor and immature monocyte marker genes, such as *S100A8, S100A9*, and *S100A12*.

NK cell-mediated cytotoxicity was suppressed in HBV cirrhosis

NK cells elicit cytotoxic effects, especially in virus-infected cells, and drive the elimination of HBV-infected hepatocytes.[26] We

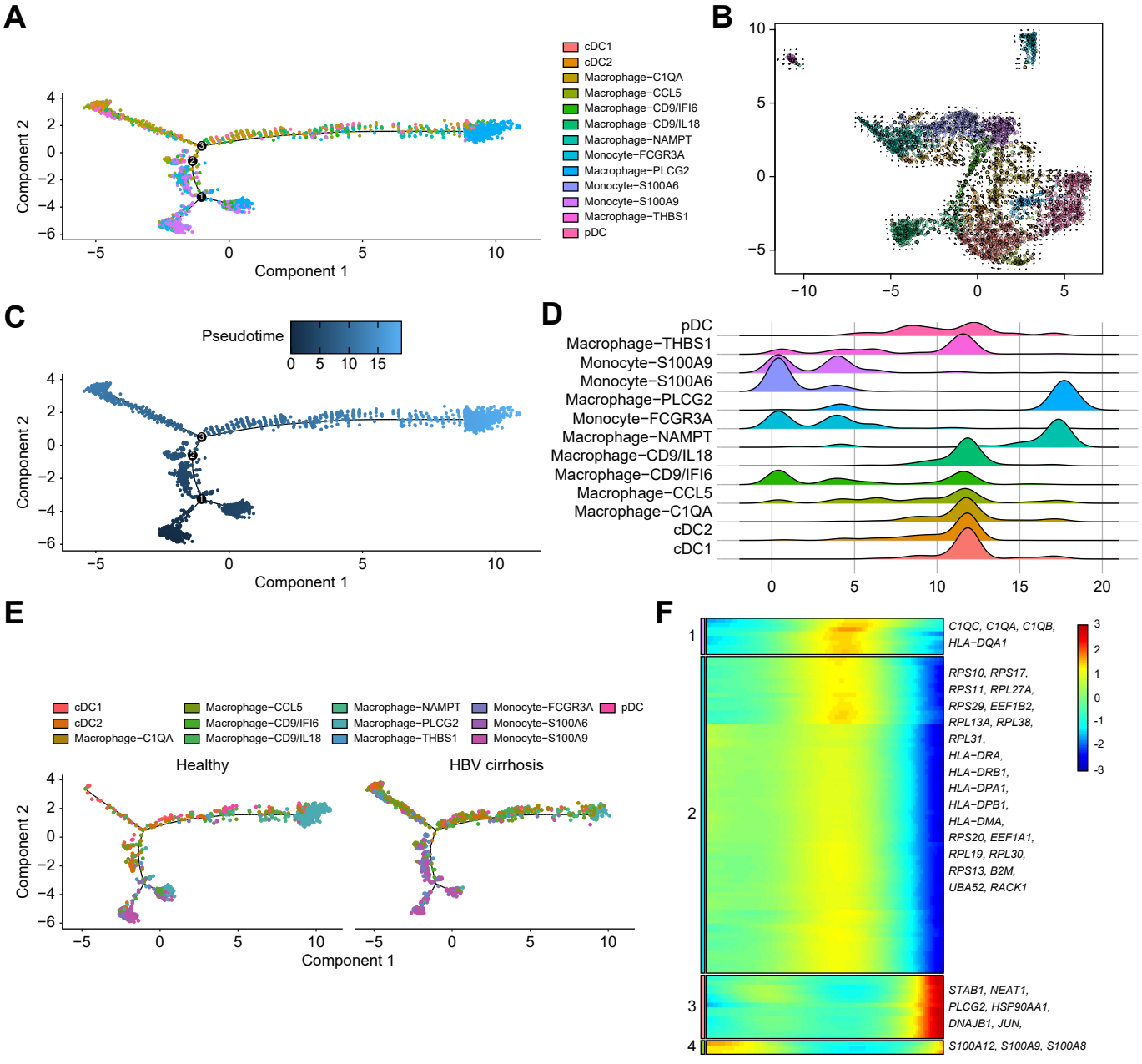

Fig. 4. Pseudo-time and RNA velocity analysis of myeloid cells. (A) Pseudo-time analysis of myeloid cells in healthy and HBV cirrhotic livers. (B) RNA velocity analysis of myeloid cells in healthy and HBV cirrhotic livers. (C) Cellular trajectory of myeloid cells. (D) The distribution of myeloid cell subtypes on the pseudo-time trajectory. (E) Pseudo-time trajectory plots of myeloid cell subtypes in healthy and HBV cirrhotic livers. (F) Gene expression dynamics of myeloid cells along the pseudo-time. Genes cluster into four sets, and each set had a specific expression profile, as depicted by a selection of characteristic genes.

performed a differential expression analysis between healthy and HBV cirrhotic NK cells (Table S6, Fig. S2A). GSEA analysis with GO annotation revealed that the functions of NK cell such as immune effector process and secretory pathways were suppressed in HBV cirrhosis samples (Fig. S2B). Similarly, with annotation pathway from KEGG database, GSEA analysis showed that NK cell mediated cytotoxicity was extensively suppressed in HBV cirrhosis samples (Fig. S2B).

Exhausted NK cells expanded in HBV cirrhosis

To further understand the roles of NK cells in the progression of HBV cirrhosis, we conducted an in-depth clustering of NK cells and identified nine distinct subclusters: NK Cell-JUNB, NK Cell-FCER1G, NK Cell-GZMH, NK Cell-TRAC, NK Cell-MYOM2, NK Cell-ANXA1, NK Cell-TIPARP, NK Cell-PLCG2, and NK Cell-GPR183 (Fig. 5A and B). Compared with healthy liver, the proportion of NK Cell-JUNB increased (p <0.001) in HBV cirrhosis (Fig. 5C and D, Fig. S2C). NK Cell-JUNB was enriched by marker genes *TNF, LAG3*, and *IL32* (Table S7). *LAG-3* represents an important indicator for NK cell exhaustion.[27] To better characterise the function of NK Cell-JUNB, the marker genes were analysed by KEGG and GO pathway enrichment analysis, with the results suggesting that NK Cell-JUNB was associated with cell–cell adhesion and regulation of T cell activation (Fig. 5E). Pseudo-time analysis was then performed to explore the differentiation trajectory of NK cells (Fig. 5F–I, Fig. S2D). Interestingly, a distinct trajectory of NK cell differentiation was observed in HBV cirrhosis samples, where NK cells at the initial stage were nearly absent.

$CD4^+$ T cell-IL7R expanded and naive B cells disappeared in HBV cirrhosis

We performed an in-depth analysis of T cell subclusters and identified nine T cell subclusters (Fig. 6A–C). Compared with the healthy liver, the proportion of $CD4^+$ T cell-IL7R increased (p <0.01) in HBV cirrhosis (Fig. 6D and E). KEGG pathway and GO enrichment analysis with $CD4^+$ T cell-IL7R marker genes suggested that the function of $CD4^+$ T cell-IL7R was associated with the ribosome, the NF-kappa B signalling pathway, and virus receptor activity (Fig. 6F). In pseudo-time analysis, $CD4^+$ T cell-IL7R exhibited a relatively mature phenotype (Fig. S3A–D).

In-depth clustering of B cells was performed to determine the potential contribution of B cells (Fig. 6G). We identified nine B cell subclusters (Fig. 6G and H). Compared with the healthy liver samples, the proportion of B cell-IGLC1 decreased (p <0.05) in HBV cirrhosis samples (Fig. 6I and J). We also performed the KEGG pathway and GO enrichment analysis of the marker genes of B cell-IGLC1. The functions of B cell-IGLC1 were associated with B cell activation and the B-cell receptor signalling pathway (Fig. 6K). In pseudo-time analysis, we found that naive B cells almost disappeared in HBV cirrhosis (Fig. S3E–H).

Discussion

Our single-cell RNA sequencing analysis revealed a unique immune ecosystem in HBV cirrhosis, characterised by an accumulation of Macrophage-CD9/IL18, Macrophage-C1QA, NK Cell-JUNB, $CD4^+$ T cell-IL7R, and a loss of B cell-IGLC1 cell clusters. Our results suggest that changes in immune cell subsets contribute, at least in part, to the progression of HBV cirrhosis. Currently, there is a lack of single-cell transcriptome profiling studies focused on immune cells in HBV cirrhosis, which limits our understanding of the underlying mechanisms involved in disease progression. Our study provides an essential advance in understanding the impact of the immune environment on HBV cirrhosis. Communication among different types of immune cells in the liver is vital for regulating local inflammatory responses and preventing the propagation of inflammatory signals. Cirrhosis disrupts the equilibrium between adaptive immunity and tolerance to pathogens, resulting in tissue damage and systemic inflammation.[3]

Myeloid cells are believed to be essential to the pathogenesis of chronic liver injury,[28] which was confirmed in our analysis. Previous studies have identified a subset of scar-associated macrophages (TREM2+CD9+) in non-hepatic cirrhosis.[4] Although we did not observe the TREM2+ subpopulation, we identified two CD9+ subpopulations of macrophages (Macrophages-CD9/IL18 and Macrophage-CD9/IFI6) in HBV cirrhosis. It is possible that variations in the aetiology of cirrhosis may contribute to differences in the characteristic genes of scar-associated macrophages. The proportion of Macrophage-CD9/IL18 and Macrophage-C1QA increased from healthy to HBV cirrhosis. The pool of hepatic myeloid cells expands dramatically after liver injury because of infiltrating monocyte-derived macrophages.[29] Accordingly, although we observed the maturation of macrophages in HBV cirrhosis, there was a significant accumulation of macrophages and loss of monocytes in HBV cirrhosis. The mobilisation of monocytes in cirrhosis has been previously described and is consistent with the notion that systemic inflammation is one of the major drivers of disease progression in cirrhosis.[3,28,30]

NK cells are a prominent subset of lymphocytes abundant in the healthy liver. Classical NK cells elicit cytotoxic effects, especially against virus-infected cells, thereby contributing to the elimination of HBV-infected hepatocytes.[26] Additionally, NK cells exhibit antibacterial activities by secreting cytokines such as interferon-gamma (IFN-γ), tumour necrosis factor alpha (TNF-α), and IL-17.[3] Understanding whether changes in NK cells within the liver of HBV cirrhosis are primarily driven by HBV infection or liver injury can be challenging. We observed an expansion of the NK cells involved in regulating T-cell activation and leucocyte cell–cell adhesion. Therefore, we propose that functional changes in NK cells may be attributed to cirrhosis-related factors rather than solely to HBV infection.

Recent research by Nkongolo *et al.*[31] uncovered an enriched population of hepatotoxic CD8+ T cells that displayed a highly activated immune signature during liver damage. In our analysis, CD8+ T cell-NKG7 possesses similar marker genes (*IFNG, GZMA, GZMK, TNFRSF9, HLA-DR, CD74, PDCD1, LAG3,* and *TIGIT*) and may represent hepatotoxic CD8+ T cells. The proportion of hepatotoxic CD8+ T cells correlated with alanine aminotransferase (ALT) levels.[31] It is worth noting that the patients with HBV cirrhosis we included had received antiviral therapy, resulting in better control of liver damage, with ALT levels increasing by a mean of 3.8-fold (Table S1). As a result, our study demonstrated a slight but not statistically significant increase in hepatotoxic CD8+ T cell-NKG7 in HBV cirrhotic liver samples (Fig. 6E).

Although our study provides valuable data for understanding the contribution of immune cells to the progression of HBV cirrhosis, a few limitations should be noted. Firstly, our data sets did not allow us to distinguish whether the observed changes are

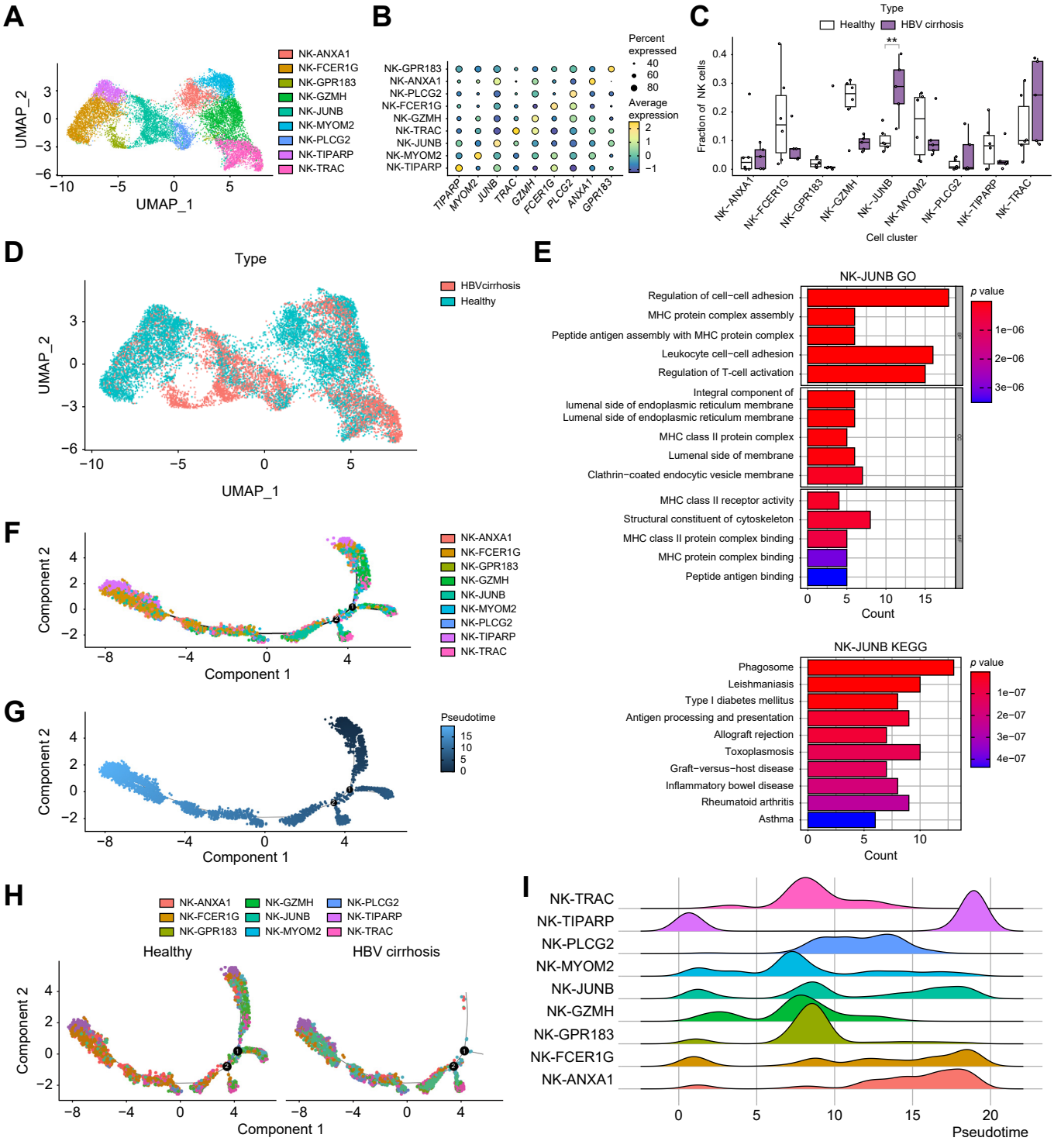

Fig. 5. The subtypes of NK cells in HBV cirrhosis and healthy liver samples. (A) Clustering analysis of NK cells. (B) Dot plot showing the marker genes in each cluster. (C) The proportion of NK cells subclusters in healthy and HBV cirrhotic liver samples. *p <0.05, **p <0.01, ***p <0.001 (Mann-Whitney U test). (D) UMAP plots of the distribution of NK cell subclusters in healthy and HBV cirrhotic livers. (E) GO and KEGG enrichment analysis of NK cell-JUNB marker genes. (F) Pseudo-time analysis of NK cells in healthy and HBV cirrhotic livers. (G) Pseudo-time of NK cells in healthy and HBV cirrhotic livers. (H) Pseudo-time analysis of NK cells in healthy and HBV cirrhotic livers. (I) The distribution of NK cell subtypes on the pseudo-time trajectory. GO, Gene Ontology; KEGG, Kyoto Encyclopaedia of Genes and Genomes; NK, natural killer; UMAP, Uniform Manifold Approximation and Projection.

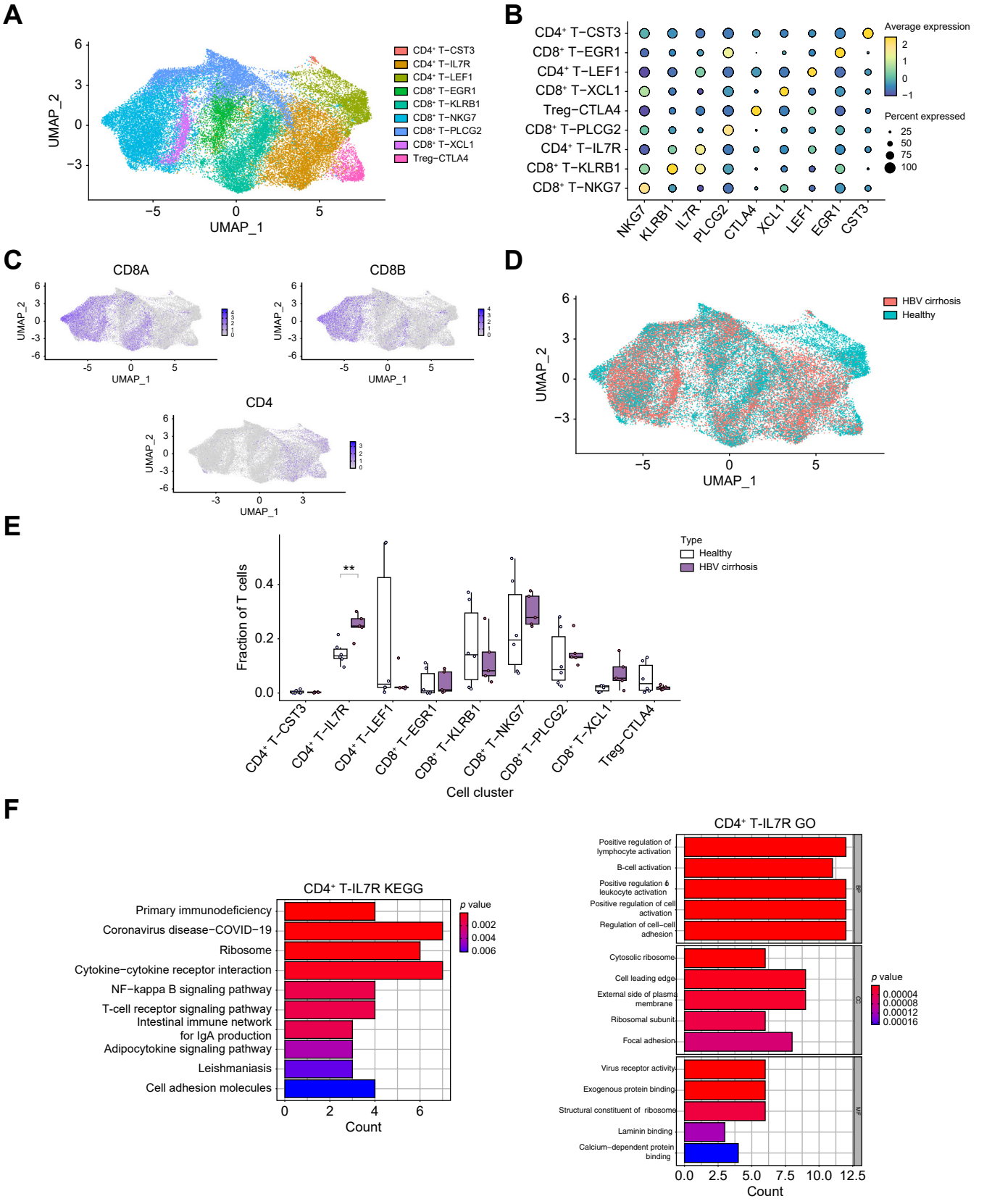

Fig. 6. The subtypes of T and B cells in HBV cirrhosis and healthy liver samples. (A) Clustering analysis of all the T cells. (B) The expression of *CD4*, *CD8A*, and *CD8B* in UMAP plot (C) Dot plot showing the marker genes in each cluster. (D) UMAP plots of the distribution of T cell subclusters in healthy and HBV cirrhotic livers. (E) The proportion of T cell subclusters in healthy and HBV cirrhotic livers. $^{**}p$ <0.01 (Mann-Whitney *U* test). (F) GO and KEGG enrichment analysis of CD4$^+$

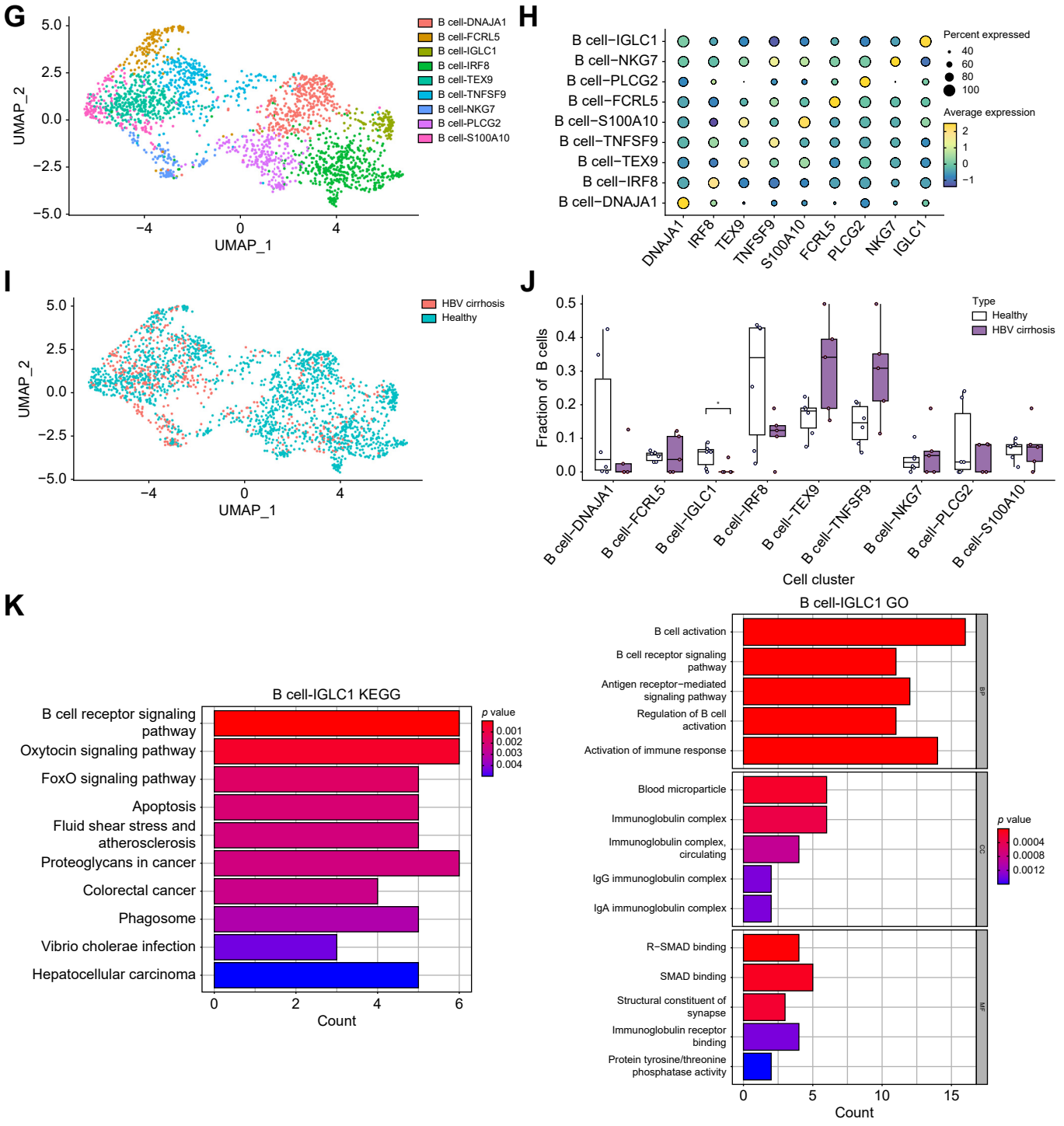

Fig. 6 (*continued*).

T cell-IL7R marker genes. (G) Clustering analysis of B cells. (H) Dot plot showing the marker genes in each cluster. (I) UMAP plots of the distribution of B cell subclusters in healthy and HBV cirrhotic liver samples. (J) The proportion of B cell subclusters in healthy and HBV cirrhotic liver samples. *p <0.05 (Mann-Whitney *U* test). (K) GO and KEGG enrichment analysis of B cell-IGLC1 marker genes. GO, Gene Ontology; KEGG, Kyoto Encyclopaedia of Genes and Genomes; UMAP, Uniform Manifold Approximation and Projection.

specifically related to the HBV infection, cirrhosis, or a combination of both. Future studies could address this by including samples from HBV-infected but non-cirrhotic livers and cirrhosis samples from non-HBV causes. Because of the challenges in collected cirrhosis tissue, the cirrhosis tissue samples we included from previously published data were from patients with hepatocellular carcinoma,[8] which may have introduced potential influence from the tumour background on the immune cells. Another limitation is the inability to identify neutrophil granulocytes in our analysis. The fragility of neutrophils during cell isolation procedures might have led to their destruction. Optimised protocols may be utilised in future study to comprehend the role of neutrophil granulocytes in HBV cirrhosis. Moreover, cirrhosis may progress to acute-on-chronic liver failure (ACLF),[32] an advanced disease stage that typically leads to distinct immune cell patterns.[30] Better understanding of the immune ecosystem will provides specific therapeutic modalities to prevent and overcome ACLF.

In conclusion, our scRNA-seq analysis of immune cells in healthy livers and HBV cirrhosis livers revealed a unique immune ecosystem associated with HBV cirrhosis. HBV cirrhosis promotes monocyte activation and differentiation and is associated with functional changes in NK cells. These findings contribute to a better understanding of the immune mechanisms underlying HBV cirrhosis and may aid in the development of novel therapeutic strategies for treatment.

Abbreviations

ACLF, acute-on-chronic liver failure; ALT, alanine aminotransferase; FACS, fluorescence-activated cell sorting; GO, Gene Ontology; KEGG, Kyoto Encyclopaedia of Genes and Genomes; NK, natural killer; PBS, phosphate-buffered saline; PCA, Principal component analysis; PI, propidium iodide; scRNA-seq, Single-cell RNA sequencing; UMAP, Uniform Manifold Approximation and Projection.

Financial support

This study was financially supported by Shenzhen Science and Technology Program (JCYJ20210324121802008), the National Natural Science Foundation of China (32270833), the Natural Science Foundation of Fujian Province (2022J01014, 2022R1001002), and the Natural Science Foundation of Xiamen City (3502Z20227164).

Conflicts of interest statement

The authors declare no conflicts of interest that pertain to this work.

Please refer to the accompanying ICMJE disclosure forms for further details.

Authors' contributions

Contributed to the conception and design of the study: QB, XH, TH, FT, CE. Provided administrative, study supervision, and obtained funding: XH, TH, FT, CE. Provided human specimens: LH. Performed experiments and substantially contributed to the acquisition of data and its analysis: QB, XH, RL, XH, HB, MH. Interpretation of data: All authors. Drafted the manuscript: QB, CE. Revised the manuscript critically for important intellectual content: All authors.

Data availability statement

Data are available at reasonable request to the corresponding author. Single-cell RNA sequencing raw data published in NCBI (RPRJNA833766).

Supplementary data

Supplementary data to this article can be found online at https://doi.org/10.1016/j.jhepr.2023.100883.

References

Author names in bold designate shared co-first authorship

[1] GBD 2017 Cirrhosis Collaborators. The global, regional, and national burden of cirrhosis by cause in 195 countries and territories, 1990–2017: a systematic analysis for the Global Burden of Disease Study 2017. Lancet Gastroenterol Hepatol 2020;5:245–266.
[2] Ligat G, Schuster C, Baumert TF. Hepatitis B virus core variants, liver fibrosis, and hepatocellular carcinoma. Hepatology 2019;69:5–8.
[3] Albillos A, Martin-Mateos R, Van der Merwe S, Wiest R, Jalan R, Alvarez-Mon M. Cirrhosis-associated immune dysfunction. Nat Rev Gastroenterol Hepatol 2022;19:112–134.
[4] Ramachandran P, Dobie R, Wilson-Kanamori JR, Dora EF, Henderson BEP, Luu NT, et al. Resolving the fibrotic niche of human liver cirrhosis at single-cell level. Nature 2019;575:512–518.
[5] Ho DW, Tsui YM, Chan LK, Sze KM, Zhang X, Cheu JW, et al. Single-cell RNA sequencing shows the immunosuppressive landscape and tumor heterogeneity of HBV-associated hepatocellular carcinoma. Nat Commun 2021;12:3684.
[6] **Zhang C**, **Li J**, **Cheng Y**, Meng F, Song JW, Fan X, et al. Single-cell RNA sequencing reveals intrahepatic and peripheral immune characteristics related to disease phases in HBV-infected patients. Gut 2023;72:153–167.
[7] Hedlund E, Deng Q. Single-cell RNA sequencing: technical advancements and biological applications. Mol Aspects Med 2018;59:36–46.
[8] Zhang Q, He Y, Luo N, Patel SJ, Han Y, Gao R, et al. Landscape and dynamics of single immune cells in hepatocellular carcinoma. Cell 2019;179:829–845 e820.
[9] **Stuart T**, **Butler A**, Hoffman P, Hafemeister C, Papalexi E, Mauck 3rd WM, et al. Comprehensive integration of single-cell data. Cell 2019;177:1888–1902 e1821.
[10] McGinnis CS, Murrow LM, Gartner ZJ. DoubletFinder: Doublet Detection in Single-Cell RNA Sequencing Data Using Artificial Nearest Neighbors. Cell Syst 2019;8:329-337 e324.
[11] La Manno G, Soldatov R, Zeisel A, Braun E, Hochgerner H, Petukhov V, et al. RNA velocity of single cells. Nature 2018;560:494–498.
[12] Gillespie M, Jassal B, Stephan R, Milacic M, Rothfels K, Senff-Ribeiro A, et al. The reactome pathway knowledgebase 2022. Nucleic Acids Res 2022;50:D687–D692.
[13] Hanzelmann S, Castelo R, Guinney J. GSVA: gene set variation analysis for microarray and RNA-seq data. BMC Bioinformatics 2013;14:7.
[14] Subramanian A, Tamayo P, Mootha VK, Mukherjee S, Ebert BL, Gillette MA, et al. Gene set enrichment analysis: a knowledge-based approach for interpreting genome-wide expression profiles. Proc Natl Acad Sci U S A 2005;102:15545–15550.
[15] Mootha VK, Lindgren CM, Eriksson KF, Subramanian A, Sihag S, Lehar J, et al. PGC-1alpha-responsive genes involved in oxidative phosphorylation are coordinately downregulated in human diabetes. Nat Genet 2003;34:267–273.
[16] Jin S, Guerrero-Juarez CF, Zhang L, Chang I, Ramos R, Kuan CH, et al. Inference and analysis of cell-cell communication using. CellChat. Nat Commun 2021;12:1088.
[17] Qiu X, Hill A, Packer J, Lin D, Ma YA, Trapnell C. Single-cell mRNA quantification and differential analysis with Census. Nat Methods 2017;14:309–315.
[18] Trapnell C, Cacchiarelli D, Grimsby J, Pokharel P, Li S, Morse M, et al. The dynamics and regulators of cell fate decisions are revealed by pseudotemporal ordering of single cells. Nat Biotechnol 2014;32:381–386.
[19] Heymann F, Tacke F. Immunology in the liver – from homeostasis to disease. Nat Rev Gastroenterol Hepatol 2016;13:88–110.
[20] Kapellos TS, Bonaguro L, Gemund I, Reusch N, Saglam A, Hinkley ER, et al. Human monocyte subsets and phenotypes in major chronic inflammatory diseases. Front Immunol 2019;10:2035.
[21] Bally I, Ancelet S, Reiser JB, Rossi V, Gaboriaud C, Thielens NM. Functional recombinant human complement C1q with different affinity tags. J Immunol Methods 2021;492:113001.
[22] Martinet J, Dufeu-Duchesne T, Bruder Costa J, Larrat S, Marlu A, Leroy V, et al. Altered functions of plasmacytoid dendritic cells and reduced

cytolytic activity of natural killer cells in patients with chronic HBV infection. Gastroenterology 2012;143:1586–1596 e1588.
[23] Golsaz-Shirazi F, Amiri MM, Shokri F. Immune function of plasmacytoid dendritic cells, natural killer cells, and their crosstalk in HBV infection. Rev Med Virol 2018;28:e2007.
[24] Jankauskas SS, Wong DWL, Bucala R, Djudjaj S, Boor P. Evolving complexity of MIF signaling. Cell Signal 2019;57:76–88.
[25] Bernhagen J, Krohn R, Lue H, Gregory JL, Zernecke A, Koenen RR, et al. MIF is a noncognate ligand of CXC chemokine receptors in inflammatory and atherogenic cell recruitment. Nat Med 2007;13:587–596.
[26] Yang PL, Althage A, Chung J, Maier H, Wieland S, Isogawa M, et al. Immune effectors required for hepatitis B virus clearance. Proc Natl Acad Sci U S A 2010;107:798–802.
[27] Roe K. NK-cell exhaustion, B-cell exhaustion and T-cell exhaustion-the differences and similarities. Immunology 2022;166:155–168.
[28] **Weiss E**, de la Grange P, Defaye M, Lozano JJ, **Aguilar F**, **Hegde P**, et al. Characterization of blood immune cells in patients with decompensated cirrhosis including ACLF. Front Immunol 2020;11:619039.
[29] Roohani S, Tacke F. Liver injury and the macrophage issue: molecular and mechanistic facts and their clinical relevance. Int J Mol Sci 2021;22:7249.
[30] **Engelmann C**, **Claria J**, **Szabo G**, **Bosch J**, **Bernardi M**. Pathophysiology of decompensated cirrhosis: portal hypertension, circulatory dysfunction, inflammation, metabolism and mitochondrial dysfunction. J Hepatol 2021;75(Suppl 1):S49–S66.
[31] Nkongolo S, Mahamed D, Kuipery A, Sanchez Vasquez JD, Kim SC, Mehrotra A, et al. Longitudinal liver sampling in patients with chronic hepatitis B starting antiviral therapy reveals hepatotoxic CD8+ T cells. J Clin Invest 2023:133.
[32] Trebicka J, Fernandez J, Papp M, Caraceni P, Laleman W, Gambino C, et al. The PREDICT study uncovers three clinical courses of acutely decompensated cirrhosis that have distinct pathophysiology. J Hepatol 2020;73:842–854.